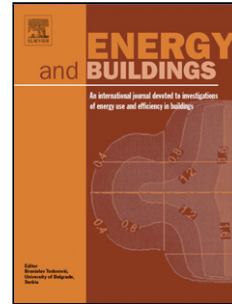


Accepted Manuscript

Title: Experimental study and performance analysis of a solar thermoelectric air conditioner with hot water supply

Author: Zhong Bing Liu Ling Zhang GuangCai Gong
YongQiang Luo FangFang Meng



PII: S0378-7788(14)00898-6

DOI: <http://dx.doi.org/doi:10.1016/j.enbuild.2014.10.053>

Reference: ENB 5436

To appear in: ENB

Received date: 24-7-2014

Revised date: 18-10-2014

Accepted date: 22-10-2014

Please cite this article as: Z.B. <ce:inter-ref id="intr0005" xlink:href="mailto:lzbljl@163.com">lzbljl@163.com</ce:inter-ref> Liu, L. Zhang, G.C. Gong, Y.Q. Luo, F.F. Meng, Experimental study and performance analysis of a solar thermoelectric air conditioner with hot water supply, *Energy and Buildings* (2014), <http://dx.doi.org/10.1016/j.enbuild.2014.10.053>

This is a PDF file of an unedited manuscript that has been accepted for publication. As a service to our customers we are providing this early version of the manuscript. The manuscript will undergo copyediting, typesetting, and review of the resulting proof before it is published in its final form. Please note that during the production process errors may be discovered which could affect the content, and all legal disclaimers that apply to the journal pertain.

Experimental study and performance analysis of a solar thermoelectric air conditioner with hot water supply

ZhongBing Liu, Ling Zhang *, GuangCai Gong, YongQiang Luo, FangFang Meng

ZhongBing Liu

E-mail address: lzbljl@163.com

College of Civil Engineering, Hunan University, Changsha, China, 410082, P.R. China

Ling Zhang

Corresponding authors: Tel: (0086) (0731) 885228641, Fax: (0086) (0731) 88822610, E-mail address:

lingzhang@hnu.edu.cn

College of Civil Engineering, Hunan University, Changsha, China, 410082, P.R. China

GuangCai Gong

E-mail address: gcgong@hnu.edu.cn

College of Civil Engineering, Hunan University, Changsha, China, 410082, P.R. China

Yongqiang Luo

E-mail address:luorosa@yeah.net

College of Civil Engineering, Hunan University, Changsha, China, 410082, P.R. China

Fangfang Meng

E-mail address: mengff2012@163.com

College of Civil Engineering, Hunan University, Changsha, China, 410082, P.R. China

22 **Abstract**

23 The condensing heat recovery in air conditioner is attractive because of its great economical and
24 environmental value. This paper presents theoretical and experimental investigations of a novel solar
25 thermoelectric air conditioner with hot water supply (STACHWS). The system can implement different
26 working modes according to the building users' requirement. Experiments were carried out under
27 different operating conditions in order to investigate the performance of the system. Results show that
28 the STEACWS can reliably be used to heat hot water without losing its cooling capacity when it is
29 controlled well in different operation conditions. The system has relatively remarkable coefficient of
30 performance (COPint) which can be as high as about 4.51 in space cooling and water heating mode.
31 When the system works as a water source thermoelectric heat pump, the coefficient of performance
32 (COP) of the system can be about 2.59 in cooling mode and 3.01 in heating mode. This simple and
33 environmentally friendly system can reduce indoor cooling and heating load and provide a continuous
34 hot water supply for householders.

35

36 Keywords: Thermoelectric; Condenser heat; Hot water supply; COP

37 **1. Introduction**

38 About 15% of global electricity energy is consumed by various air conditioning and refrigeration
39 processes, and 59% of the energy consumption in commercial and household buildings is attributed to
40 air conditioning and water heating systems in 2011 [1]. Building energy conservation is of great
41 significance nowadays. Usually, the heat of condensation from air conditioners will directly be
42 discharged to the outside. This process is blamed for waste of energy as well as the thermal pollution to
43 the outside environment. On the other hand, in order to meet building hot water supply, an external
44 electrical or gas-fired boiler must operate all-day long. In this situation, the condensing heat in air
45 conditioners has been attracting significant attention.

46 Many methods have been adopted on condensing heat recovery in vapor-compression air conditioning
47 systems for condenser heat recovery. For instance, phase change material was used to restore the heat
48 of the air conditioning system by Zhang et al. [2]. In addition, a helical heat exchanger was studied
49 for heat recovery system by Yi et al. [3]. Because of its great economical and environmental value, the
50 condensing heat recovery in vapor compression air conditioning systems had been applied to many
51 engineering projects [4-6]. However, the traditional vapor compression system has some disadvantages:
52 (1) To meet the energy consumption of traditional vapor compression systems, natural resources are
53 burned to generate electricity, which causes greenhouse effect and to exacerbate a lot of pollution on
54 the earth. (2) The Freon in vapor compression system once leaked, will cause irreversible damage to
55 the ozone sphere and make life suffer from ultraviolet radiation. Hence, a novel solar thermoelectric air
56 conditioner integrated water heater system is proposed. The system uses thermoelectric modules
57 powered by solar energy for heating hot water and cooling room simultaneously, therefore the system
58 can reduce the utilization of traditional energy source, without doing any harm to the environment.

59 Thermoelectric material can be used in two major operating models: thermoelectric generator [7] and
60 thermoelectric cooler (TEC) [8-9]. Thermoelectric cooler systems have no mechanical moving parts
61 and do not employ working fluids, which can transfer heat from the cold side of the modules to the
62 hotter side with consumption of electricity [10-11]. Due to the advantages such as high reliability, low
63 weight, and flexibility in packaging and integration, the TEC systems are regarded as clean and active
64 cooling methods, which have been widely used in military, aerospace, instrument, and industrial
65 products [12-15]. In addition, due to their bright prospect, some thermoelectric applications are likely
66 to be commercialized, such as air conditioners for domestic, thermoelectric ventilator, thermoelectric
67 cooled ceiling, etc, which compete with vapor compression based applications [16-18]. Moreover,
68 thermoelectric cooler system can be powered directly by a photovoltaic (PV), and no AC/DC inverter is
69 needed. Therefore, it is recognized that the thermoelectric coolers and the solar cells combined system
70 can be used for the air-conditioning applications, and the technology actually meets the demand for
71 energy conservation and environment protection [19].

72 The main significance of this paper is to study the novel solar thermoelectric air conditioner integrated
73 water heater technology in the application of low-carbon buildings. Compared with traditional
74 thermoelectric air conditioner, the system can cool the room with thermoelectric powered by PV, at the
75 same time, the water can be heated by the hot side of the TEC modules. Therefore, thermal energy can
76 be recovered from the hot side of the thermoelectric module. Moreover, the system can work as a water
77 source thermoelectric heat pump for space cooling in summer and space heating in winter. This system
78 can reduce indoor cooling and heating load and provide hot water supply for uses. Thus, the novel
79 system can be applied in a vast field.

80 **2. The system working principle**

81 Fig.1 illustrates the novel solar thermoelectric air conditioner with hot water supply system proposed
82 for space cooling and hot water supply. As shown in Fig.1, the solar thermoelectric air conditioner with
83 hot water supply (STACHWS) is divided into three parts: (1) the air part, (2) the TEC modules part,
84 and (3) the water part. The PV system can provide a constant DC power supply during daytime, while
85 batteries can provide power to the STEACWH system at night. According to the applications, the
86 STEACWH system can be classified in the following operating modes:
87 (1) Space cooling and water heating mode: this mode is used in summer when space cooling and hot
88 water are both required. When the system begins to work, the water tank is filled full with water. The
89 return air is cooled down when it flows through heat exchangers into the indoor environment. At the
90 same time, the water is heated up in the water tank by the heat exchanger on the other side of the TEC
91 modules. Therefore, thermal energy can be recovered from the hot sides of TEC modules.

92
93
94 Fig.1. The working principle of the solar thermoelectric air conditioner with hot water supply
95 (2) Space cooling: This mode is the normal thermoelectric cooling mode for space cooling. Different
96 from space cooling and water heating mode, the system work as a water source thermoelectric heat
97 pump and the heat of the hot side of the thermoelectric modules is dissipated by flow water. The air is
98 cooled down when it flows through heat exchangers moving into the indoor environment for space
99 cooling.

100 (3) Space heating: In winter, revise the direction of current inputting the thermoelectric modules and
101 then the heating side and cooling side reverse. The heat of the cold side of the thermoelectric modules
102 is dissipated by the flow water. Then the system can work as a water source thermoelectric heat pump.
103 The air is heated up when it flows through heat pipe exchangers moving into the indoor environment
104 for space heating.

105 **3. Theory of computer model**

106 3.1 Mathematic model

107 Fig.2 depicts a prototype thermoelectric model developed for the design and analysis of STACHWS
 108 system. The TE modules are sandwiched between the hot and cold side heat exchangers. Heat is either
 109 absorbed or released at the junction when an electrical current is passed through the junction of
 110 dissimilar conductors. Reversing the direction of the current changes the direction of the heat flow.

111

112 Fig.2.Schematic diagram and simplified model of STACHWS

113 The following formulate show relations for the different parameters in the STACHWS system, and the
 114 formulate are useful for setting up the model.

115 Inside heat sink heat balance equations:

116 $T_c = T_a - Q_c R_c$ (for cold side) (1)

117 $T_h = Q_h R_h + T_w$ (for hot side) (2)

118 In the above equations, the air side heat sink thermal resistance R_c is 0.3 W^{-1} (when the air velocity
 119 is 3.2 m/s) and R_h is 0.2 W^{-1} in space cooling and water heating mode, and when the system work as
 120 a water source thermoelectric heat pump, the thermal resistance of air side heat sink R_c is 0.3 W^{-1}
 121 (when the air velocity is 3.2 m/s) and the water side heat sink thermal resistance R_h is $0.18 \text{ /W} \text{ W}^{-1}$
 122 (when the flow rates of water is 2 L/min) in cooling mode. These values were obtained by tested.

123 Average temperature of the hot side and cold side of the thermoelectric modules:

124 $T_m = (T_h + T_c)/2$ (3)

125 Thermoelectric material seebeck coefficient of:

126
$$a = \frac{N_{new}}{71} \times \frac{(\alpha_1 T_h + \alpha_2 T_h^2/2 + \alpha_3 T_h^3/3 + \alpha_4 T_h^4/4) - (\alpha_1 T_c + \alpha_2 T_c^2/2 + \alpha_3 T_c^3/3 + \alpha_4 T_c^4/4)}{T_h - T_c} \quad (4)$$

127 $\alpha_1 = 1.33450 \times 10^{-2}$,

128 $\alpha_2 = -5.37574 \times 10^{-5}$

129 $\alpha_3 = 7.42731 \times 10^{-7}$

130 $\alpha_4 = -1.27141 \times 10^{-9}$

131 Resistivity of thermoelectric material:

132
$$r = \frac{N_{new}}{71} \times \frac{6}{I_{new}} \times \frac{(r_1 T_h + r_2 T_h^2/2 + r_3 T_h^3/3 + r_4 T_h^4/4) - (r_1 T_c + r_2 T_c^2/2 + r_3 T_c^3/3 + r_4 T_c^4/4)}{T_h - T_c} \quad (5)$$

133 $r_1 = 2.08317$

134 $r_2 = -1.98763 \times 10^{-2}$

135 $r_3 = 8.53832 \times 10^{-5}$

136 $r_4 = -9.03143 \times 10^{-8}$

137 Thermal conductivity:

138
$$k = \frac{N_{new}}{71} \times \frac{I_{new}}{6} \frac{(k_1 T_h + k_2 T_h^2/2 + k_3 T_h^3/3 + k_4 T_h^4/4) - (k_1 T_c + k_2 T_c^2/2 + k_3 T_c^3/3 + k_4 T_c^4/4)}{T_h - T_c} \quad (6)$$

139 $k_1 = 4.76218 \times 10^{-1}$

140 $k_2 = -3.89821 \times 10^{-6}$

141 $k_3 = -8.64864 \times 10^{-6}$

142 $k_4 = 2.20869 \times 10^{-8}$

143 The amount of heat absorber at the cold junction (Q_c) and the heat dissipated at the hot junction (Q_h) is
144 given by [20-21]:

145
$$Q_c = aI(T_c + 273.15) - \frac{1}{2} I^2 r - k(T_h - T_c) \quad (7)$$

146
$$Q_h = aI(T_h + 273.15) + \frac{1}{2} I^2 r - k(T_h - T_c) \quad (8)$$

147 Where I is the operating current; T_c is the cold side temperature and T_h is the hot side temperature; R is
148 the thermoelectric module's electrical resistance ($R = 2N\sigma / G$); S is the thermoelectric module's
149 electrical resistance; and K is the thermoelectric module's thermal conductance ($K = 2NkG$). S , R and K
150 are the temperature dependent parameters. N refers to the total number of thermoelectric elements used
151 in each module. G is the geometric factor, and a , σ , K are the material properties for the specific the

152 type of the TE element. The values of S , R , and K are varying according to the average temperature of
 153 the thermo element T_m , the relations are supplied by [21].

154 The heat balance of the storage tank is calculated by:

$$155 Q_{\text{tank}} = C_{\text{pw}} M_w \Delta T \quad (9)$$

156 Where Q_{tank} is the gained heat of the water in storage tank, C_{pw} is the specific heat capacity of water
 157 which is 4200 kJ/(kg k) , M_w stands for the mass of water in storage tank, ΔT represents the water
 158 temperature variation.

159 The heat balance between the storage tank and environment is calculated by:

$$160 Q_{\text{loss}} = K_1 S_1 (T_w - T_e) / L_1 \quad (10)$$

161 Where $Q_{\text{loss-te}}$ is the heat transfer between the storage tank and environment, K_1 is the heat transfer
 162 coefficient of insulation material, which is 0.03 W/k.m , S_1 is the area of storage tank, which is 0.6 m^2 ,
 163 T_w is the water temperature in the storage tank. L_1 is the thickness of insulation, which is 1.5 cm .

164 The equation of fan is provided by:

$$165 P_{\text{fan}} = U_{\text{fan}} I_{\text{fan}} \quad (11)$$

166 Where P_{fan} is the power of fan, U_{fan} is the operating voltage of fan, and I_{fan} is the operating current of
 167 fan.

168 An integrated coefficient of performance (COP_{int}) is defined to estimate the energy utilization of the
 169 integrated system. The energy utilization of the system includes the effective cooling capacity Q_c and
 170 the effective heating water capacity, Q_h .

$$171 Q_{\text{hw}} = Q_h - Q_{\text{loss}} \quad (12)$$

$$172 \text{COP}_c = \frac{Q_c}{W + P_{\text{fan}}} \quad (13)$$

173 $COP_h = \frac{Q_h}{W + P_{fan}}$ (14)

174 $COP_{int} = \frac{Q_c + Q_{hw}}{W + P_{fan}}$ (15)

175 $COP_{int-w} = \frac{Q_{hw}}{W + P_{fan}}$ (16)

176 Where W is the power of thermoelectric modules.

177 3.2 Structure of the model

178 In this work, a thermoelectric air conditioner with hot water supply (STACHWS) technology system is
 179 proposed. In order to better understand the performance of the system, a simulation model based on the
 180 equations in section 3.1 is set up to estimate the performance of the thermoelectric air conditioner with
 181 hot water supply. The flow chart of this model is shown in Fig.3.

182

183 Fig.3.Flow chart of the system simulation model

184 **4. Experimental testing**

185 The STACHWS prototype was fabricated and tested in an environmental chamber in the laboratory. It
 186 comprised two heat pipe sinks, twenty-four thermoelectric modules, a water tank and cool fan as shown
 187 in Fig.3. The TE modules are sandwiched between two heat pipe sinks. Thermal insulating material
 188 was filled on the gap between on the two heat sinks. The Thermal conducts between all contacting
 189 surfaces were improved by applying thermal grease. The water tank is 600 mm×300 mm×200mm. The
 190 water tank is made of Zinc Plating, which is 1.5mm thick. In order to reduce heat dissipation, the wall
 191 of water tank is packaged by 60mm thick insulation materials. The TE modules used in this study were
 192 purchased from FERROTEC Corporation [18]. The TE modules type is 9500/127/060 B. The power of
 193 the ventilator is 18 W and the air volume is 120m³/h.

194

195 Fig.4. Schematic diagrams of the experimental apparatus.

196 The temperature were recorded by means of PT100 using an Envada EN880 modular paperless process
197 recorder logger with temperature sensors. The temperature sensor accuracy is ± 0.1 . At present, a
198 DC power supply was used to power the TE module. The operating voltage and current can be read by
199 the LCD display. In the experimental studying the thermoelectric system's performance characteristics,
200 the air temperature of the lab room was maintained at 26 in summer mode and 18 in winter mode.
201 The tests were carried out in space cooling and water heating mode, space cooling mode and heating
202 mode. In space cooling and water heating mode, the water tank is filled with water. And the heat of the
203 hot side of the thermoelectric modules is dissipated by the flow water when the system works as a
204 water source thermoelectric heat pump.

205 **5. Results and analysis**206 **5.1 Simulation and experimental results**

207 In this section, simulation results and experimental results under different operation conditions will be
208 presented and discussed to analyze the performance of the STACHWS system. The indoor environment
209 temperature and humidity is set up as constant in the simulation process in summer and winter mode.
210 As a result, the temperature of the air coming into the STACHWS is taken as constants. The experiment
211 results for the hot and cold side temperature varied with the temperature of hot water compared with
212 the simulation dates in space cooling and water heating mode are shown in Fig.5. It can be observed
213 that the hot side temperature (Th) keeps increasing rapidly with the hot water temperature increase, at
214 the same time, the cold side temperature (Tc) increases simultaneously but more slowly compared with
215 the hot side temperature (Th) , therefore the temperature difference between the hot and cold sides
216 becomes larger.

217

218 Fig.5.The hot and cold side temperature under different water temperature in space cooling and water
219 heating mode

220
221 Fig.6 presents cooling and heating capacity of the system under an operating voltage of 5V with the hot
222 water temperature increases in space cooling and water heating mode. As can be seen, the cooling and
223 heating capacity of the system was relatively high and decrease as the water temperature increase. The
224 cooling and heating capacity are 430W and 652W separately when the water temperature is 20 $^{\circ}\text{C}$, and
225 when the water temperature increase to 42 $^{\circ}\text{C}$, the cooling and heating capacity are 178W and 353W.
226 The reason behind this phenomenon was that the temperature difference between the hot and cold sides
227 increases with the water temperature increases as shown in Fig5. According to the equation 1, the
228 higher the temperature difference between the cold and hot sides, the lower the cooling and heating
229 capacity is.

230
231 Fig.6. Cooling and heating capacity under different water temperature in space cooling and water
232 heating mode

233
234 Fig.7 presents the COP_{int,w} and COP_{int} of the system under an operating voltage of 5V with the water
235 temperature increases in space cooling and water heating mode. As shown in Fig.7, the simulations and
236 experiment results share the same trend and regularity in space cooling and water heating mode. As can
237 be seen, the COP_{int,w} and COP_{int} increased first to its maximum, and then decreased gradually when
238 the water temperature increased as shown in Fig7. The maximum COP_{int} is 4.6. It is indicated that the
239 system require less electrical energy and works more efficiently with lower water temperature in space
240 cooling and water heating mode. The COP_{int,w} decreased from 2.71 to 1.82 when the hot water
241 temperature increased from 20 $^{\circ}\text{C}$ to 42 $^{\circ}\text{C}$. It was conclude that the COP_{int,w} played an important role
242 in COP_w of the prototype in space cooling and water heating mode.

243

244 Fig.7. COP under different water temperatures in space cooling and water heating mode

245

246 Space cooling mode is usually used in summer. Different from space cooling and water heating mode,
 247 the hot side of the thermoelectric system absorbed heat from flow water in space cooling mode. As a
 248 result, the performance of the system can be improved, as the heat dissipation on the hot sides of the
 249 TEC modules is better than in space cooling and water heating mode. The flow rate of heat medium on
 250 hot side is 2L/min. Fig.8 presents the cooling capacity and COP_c of the system under an operating
 251 voltage of 4V with different water inlet temperature in space cooling mode. The lower water inlet
 252 temperature contributes the higher the performance of the system. As can be seen, the maximum COP_c
 253 of the system is 2.4 when the system works stably under the water inlet temperature of 12 °C.

254

255 Fig.8. Cooling capacity and COP_c under different water inlet temperature in space cooling mode

256

257 In winter, revise the current direction inputting the thermoelectric modules and the cold side of the
 258 thermoelectric system absorbed heat from the flow water, then the system work as a water source
 259 thermoelectric heat pump. The flow rate of heat medium on cold side is 2L/min. Fig.8 shows the
 260 heating capacity and COP of simulations and experiments under different water inlet temperature when
 261 the voltage is 4V. The results were recorded when the system works stably. As shown in Fig8, the water
 262 inlet temperature has an important effect on the performance of the system in space heating mode. The
 263 heating capacity and the COP of the system decreased when the water inlet temperature increased. The
 264 COP_h can be reached at 3.05 when the water inlet temperature is 24 °C, which is more efficient than
 265 electric heater and also is larger than COP of 2.6 which is required the performance of air-source heat
 266 pump air conditioner in China.

267

268 Fig.9. Heating capacity and COP_h under different water temperature in space heating mode

269

270 As shown in Figs.5-9, there is certain difference between modeling and experimental results. The
 271 values of theoretical coefficient of performance are always higher than the experiment data. Table 1
 272 shows the values of hot and cold side temperature for the modeling and experimental data and the
 273 relative deviation. There is certain difference between modeling and experimental results due to a
 274 number of factors, such as the measurement inaccuracy, the material property difference and the
 275 difference between ideal and actual thermal resistance of heat exchangers. It also can be seen from
 276 Table 1, the relative deviations between the simulations and experiments are small, it indicated that the
 277 simulations result and the experiment results are agree well with each other.

278

279 Table 1 Comparison of the hot and cold side temperature for modeling and testing

280 5.2. System optimization

281 The STACHWS system can be designed based on two principles, namely, the principle of maximized
 282 COPint, which is adopted in the design of STACHWS system and the principle of maximized cooling
 283 and heating capacity. The impact of electric current on COPint is shown in Fig.10. As can be seen, there
 284 is an optimum current (I_{op}) that let COPint have the maximum value. I_{op} is relevant to the water
 285 temperature. Larger water temperature leads to a high I_{op} but a low COPint. When the STACHWS
 286 system work in space cooling and water heating mode, it can be observed that, there is an optimum
 287 COPint existing when electric current is about 0.8 to 1.4A under different water temperature, larger or
 288 lower current rate is unhelpful to improve COPint. In space cooling and water heating mode, it can
 289 change the current of the STACHWS system under different water temperature in order to get a better
 290 performance.

291

292

293 Fig. 10 Impact of electric current on COPint

294 **6. Discussion**

295 According to the test and simulation results, the maximum COP of the novel solar thermoelectric air
296 conditioner with hot water supply is 2.59 in cooling mode and 3.01 in heating mode when the system
297 works as a water source thermoelectric heat pump. And when the system work in space cooling and
298 water heating mode, the COPint is decreases from 4.51 to 2.74 when the hot water temperature increase
299 from 20 °C to 42 °C. This value is higher than conventional split-type air conditioner (2.4 in average)
300 and is more efficient than an electrical heating device, therefore it becomes more attractive. The TEC
301 system performance is closely related to the figure of merit of thermoelectric materials, ZT, the TE
302 modules used in this paper has a ZT of 0.61, which is not high considering the progress of TE
303 technology. It is achievable since the latest quantum well materials have a ZT as high as 2.4 at 300 K
304 [22], and when TE materials that have a ZT = 2, the COP of thermoelectric air conditioner can reach
305 that of vapor compression coolers in climate-control applications [23]. Moreover, the performance of
306 the STACHWS can be further improved by optimizing design and fabrication based on experimental
307 data.

308 In the present experiments, the STACHWS system is powered by a DC power supply, this power will
309 be replaced by a PV system in further studies. In daytime, the PV systems receive solar energy and turn
310 it into electric power supplied to thermoelectric modules. If the electric power production is larger
311 enough, the surplus power can be accumulated in storage battery besides driving the STACHWS
312 system. Moreover, if the PV systems cannot produce enough electric power, for example, in rainy days,
313 the storage battery may offer a makeup. The PV system and battery is controlled by an auto-switcher,
314 which can play a role to maintain the energy conversion process in most optimized way.

315

316 **7. Conclusions**

317 In this study, a solar thermoelectric air conditioner with hot water supply (STACHWS) is proposed and
 318 tested. The system can shift flexibly between different working modes according to the building users'
 319 requirement. The system can be powered using renewable energies, in particular PV system, which
 320 produces DC electricity. Experiments were carried out under different operating conditions in order to
 321 investigate the performance of the system. The conclusions reached in the present study are listed as
 322 follows:

323 (1) The simulations result and the experiment results are agree well with each other. It indicated that the
 324 system could reliably be used to heat hot water without losing its cooling capacity.

325 (2) The results show that the performance of the STACHWS system is strongly influenced by water
 326 temperature. The COPint decrease as the water temperature increase in space cooling and water heating
 327 mode. The system has relatively large coefficient of performance (COPint) which can be as high as
 328 about 4.51 when the water temperature of 20 $^{\circ}\text{C}$ and 2.74 at water temperature of 42 $^{\circ}\text{C}$.

329 (3) When the system works as a water source thermoelectric heat pump, the system works more
 330 efficiently with lower water inlet temperature in cooling mode and higher water inlet temperature in
 331 heating mode. The coefficient of performance (COP) of the system can be about 2.59 when the inlet
 332 water temperature of 12 $^{\circ}\text{C}$ and 1.86 at the inlet water temperature of 28 $^{\circ}\text{C}$ in cooling mode. In heating
 333 mode, the COP of the system is 3.01 when the water inlet temperature is 24 $^{\circ}\text{C}$ and 2.01 when the water
 334 temperature of 8 $^{\circ}\text{C}$.

335 (4) The performance of the system can be improved by the optimization operating voltage, reducing the
 336 heat transfer resistance, especially the heat transfer resistance on the hot side of the thermoelectric
 337 modules. The thermoelectric module used in this work has a figure of merit ZT value of 0.65, and if the
 338 TE modules used in this paper has a ZT of 0.61, which is not high considering the progress of TE

339 technology. And when TE materials that have a $ZT = 2$, the COP and energy conservation ratio of the
 340 system could be further increased.

341 **Acknowledgements**

342 The work described in this paper was sponsored by the National Natural Science Foundation of China
 343 (Grant No.51178170), Collaborative Innovation Center Building Energy Conservation & Environmental
 344 Control of Hunan Province. The supports are gratefully acknowledged.

345

346 **Abbreviates of parameters:**

347 COP_{int} – the integrated coefficient of performance is defined to estimate the energy utilization of the
 348 integrated system

349 $COP_{int,w}$ – it is that the COPint is simplified when the cooling capacitive is equal to zero

350 T_w – the water temperature (°C),

351 T_{wi} – the water inlettemperature of the system (°C),

352 COP_c – system cooling coefficient of performance,

353 COP_h – system heating coefficient of performance,

354 I -applied current of TE module (A),

355 Q_c –The cooling capacity of the TE modules at the cold junction (W),

356 Q_h –The heating capacity of the TE modules at the hot junction (W),

357 T_c - cold side of temperature of TE module(°C),

358 T_h - hot side temperature of TE module (°C),

359 T_i – air temperature of indoor (°C),

360 ΔT -temperature difference of TE module (°C),

361 V -applied voltage of TE module (V),

362 **References:**

363 [1] 2011 building energy data book, U.S. Department of Energy, 2012.

364 [2] Xuelai Zhang, Shuxuan Yu, Mei Yu, Yuanpei Lin, Experimental research on condensing heat
365 recovery using phase change material, *Applied thermal engineering*17(17-18)(2011)3736-3740.

366 [3] X. Yi, W.L. Lee, The use of helical heat exchanger for heat recovery domestic water-cooled air
367 conditioners, *Energy Conversion and Management* 50 (2) (2009) 240–246.

368 [4] Ming Liu Jiang, Jing Yi Wu, Yu Xiong Xu, Ru Zhu Wang, Transient characteristics and
369 performance analysis of a vapor compression air conditioning system with condensing heat
370 recovery, *Energy and buildings*42 (2010)2251-2257.

371 [5] Jie Jia, W.l. Lee, Applying storage-enhanced heat recovery room air-conditioner (SEHRAC) for
372 domestic water heating in residential buildings in Hong Kong, *Energy and buildings*
373 78(2014)132-142.

374 [6] Guangcai Gong, Feihu Chen, Huan Su, Jian yong Zhou, Thermodynamic simulation of
375 condensation heat recovery characteristics of a single stage centrifugal chiller in a hotel, *Applied*
376 *energy*91(1)(2012)326-333.

377 [7] Minfeng Zhou, Yongling He, Yanmin Chen, A heat transfer numerical model for thermoelectric
378 generator with cylindrical shell and straight fins under steady-state conditions, *Applied thermal*
379 *engineering*68(1-2)(2014)80-91.

380 [8] Jing-Hui Meng, Xiao-Dong Wang, Xin-Xin Zhang, Transient modeling and dynamic
381 characteristics of thermoelectric cooler, *Applied Energy* 108 (2013) 340-348.

382 [9] M.K. Russel, D. Ewing, C.Y. Ching, Characterization of a thermoelectric cooler based thermal
383 management system under different operating conditions, *Applied Thermal Engineering* 50(2013)
384 652-659.

385 [10] Riffat SB, Ma X, Thermoelectric: a review of present and potential applications, *Applied
386 Thermal Engineering* 23 (8) (2003)913-935.

387 [11] Di Liu, Fu-Yun Zhao, Guang-fa Tang, Active low-grade energy recovery potential for building
388 energy conservation, *Renewable and Sustainable Energy Reviews*. 14(2010)2736-2747.

389 [12] Tsung-chieh cheng, Chin-Hsiang Cheng, Zhu-Zin Huang. et al, Development of an
390 energy-saving module via combination of solar cells and thermoelectric coolers for green
391 building applications, *Energy*36(1)(2011)133-140.

392 [13] Xu Xu, Steven Van Dessel, Evaluation of a prototype active building envelope window-system,
393 *Energy and Buildings*40(2) (2008)168-174.

394 [14] Y.J. Dai, R.Z. Wang, L. Ni, Experimental investigation and analysis on a thermoelectric
395 refrigerator driven by solar cells, *Solar Energy Materials & Solar Cells* 77(4) (2003)377–391.

396 [15] Wei He, Jinzhi Zhou, Jingxin Hou, Chi Chen, Jie Ji, Theoretical and experimental investigation
397 on a thermoelectric cooling and heating system driven by solar, *Applied Energy* 107
398 (2013)89-97.

399 [16] Tianhe Han, Guangcai Gong, Zhongbin Liu, ling Zhang, Optimum design and experimental
400 study of a thermoelectric ventilator, *Applied Thermal Engineering* 67 (1-2) (2014) 529-539.

401 [17] Y.W,Kim, J.Ramousse, G.Faisse et al, Optimal sizing of a thermoelectric heat pump (THP) for
402 heating energy-efficient buildings, *Energy and buildings* 70(2014)106-116.

403 [18] ZhongBing Liu, Ling Zhang, GuangCai Gong, Experimental evaluation of a solar thermoelectric

404 cooled ceiling combined with displacement ventilation system, Energy Conversion and
405 Management87(2014).

406 [19] Hongxia Xi, Lingai Luo, G Fraisse, Development and applications of solar-based thermoelectric
407 technologies, Renewable and Sustainable Energy Reviews11(5)(2007)923-936.

408 [20] D.S. XU, Thermoelectric Refrigeration and Its Application, Shanghai Jiao tong University Press,
409 Shanghai, 1998.

410 [21] Forrotec Corporation, 2014, <http://www.ferrotec.com.cn>.

411 [22] A. J. Minnich, M. S. Dresselhaus, Z. F. Ren, and G. Chen, Bulk nanostructured thermoelectric
412 materials: current research and future prospects, Energy & Environmental
413 Science2(2009)466-479.

414 [23] J.P. Heremans. Low-Dimensional Thermoelectricity, Acta physica Polonica A108 (2005)
415 609-634.

416

417 **Figures captions**

418 Table 1 Comparison of the hot and cold side temperature for modeling and testing

419 Fig.1.The working principle of the solar thermoelectric air conditioner with hot water supply

420 Fig.2.Schematic diagram and simplified model of STACHWS

421 Fig.3.Flow chart of the system simulation model

422 Fig.4. Schematic diagrams of the experimental apparatus.

423 Fig.5.The hot and cold side temperature under different water temperature in space cooling and
424 water heating mode

425 Fig.6. Cooling and heating capacity under different water temperature in space cooling and water
426 heating mode

427 Fig.7. COP under different water temperatures in space cooling and water heating mode

428

429 Fig.8. Cooling capacity and COPc under different water inlet temperature in space cooling mode

430 Fig.9. Heating capacity and COPh under different water temperature in space heating mode

431 Fig. 10 Impact of electric current on COPint

432

432

433

Table 1 Comparison of the hot and cold side temperature for modeling and testing

Operating mode	Operating condition	T _h ()			T _c ()		
		Simulation	Experiment	δ(%)	Simulation	Experiment	δ(%)
Space cooling and water heating	20 (T _w)	25.6	26.5	-3.5	15.0	14.8	1.3
	42 (T _w)	45.1	45.5	-0.9	21.4	21.2	0.9
Space cooling	12 (T _{wi})	18.9	19.3	-2.1	14.8	14.4	2.7
	24 (T _{wi})	29.2	29.4	-0.7	18.2	17.6	3.3
Space heating	16 (T _{wi})	27.4	27.8	-1.5	12.6	12.5	0.8
	24 (T _{wi})	29.6	30.2	-2.0	19.6	19.4	1.0

434

435

435 ►A novel solar thermoelectric air conditioner with hot water supply system was proposed.

436 ►A simulation model for thermoelectric system was developed.

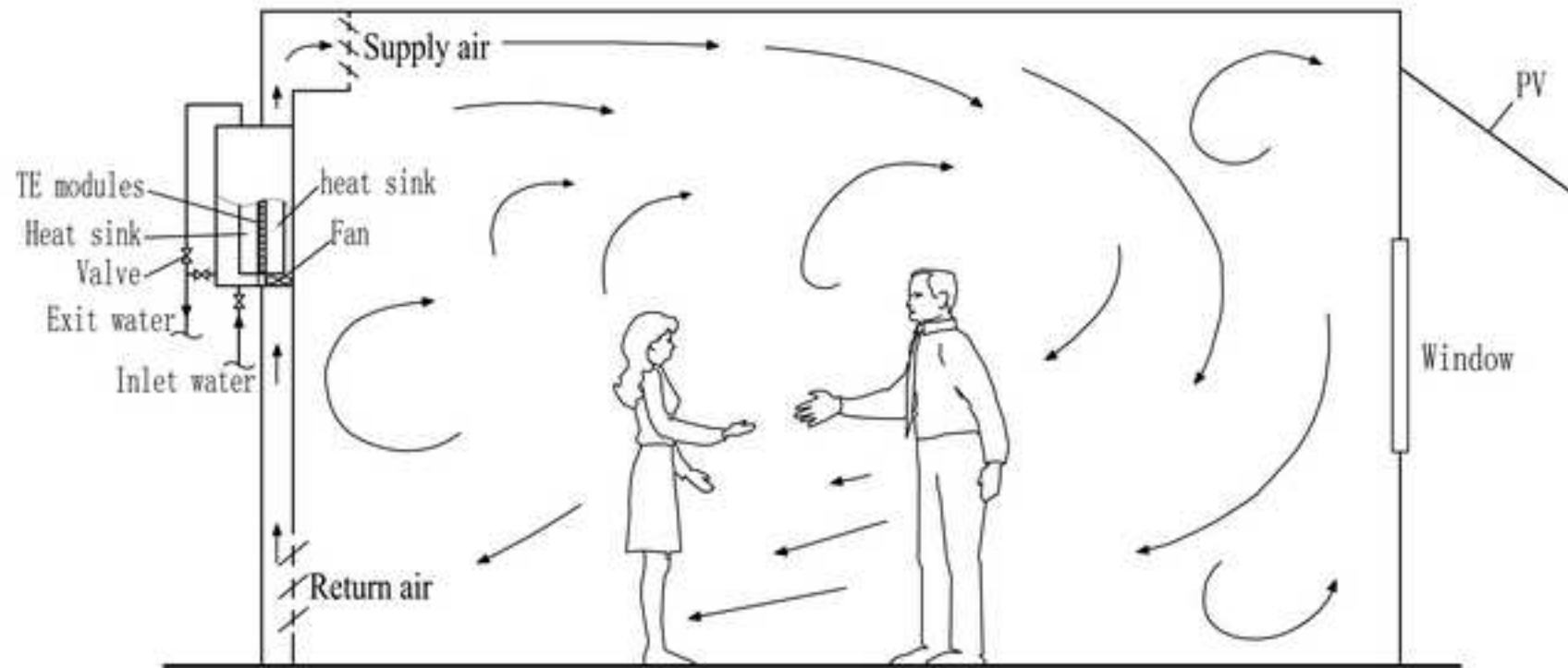
437 ►A simulation program and experiments are conducted to identify the performance.

438 ►The coefficient of performance which can be as high as about 4.51 in space cooling and water heating

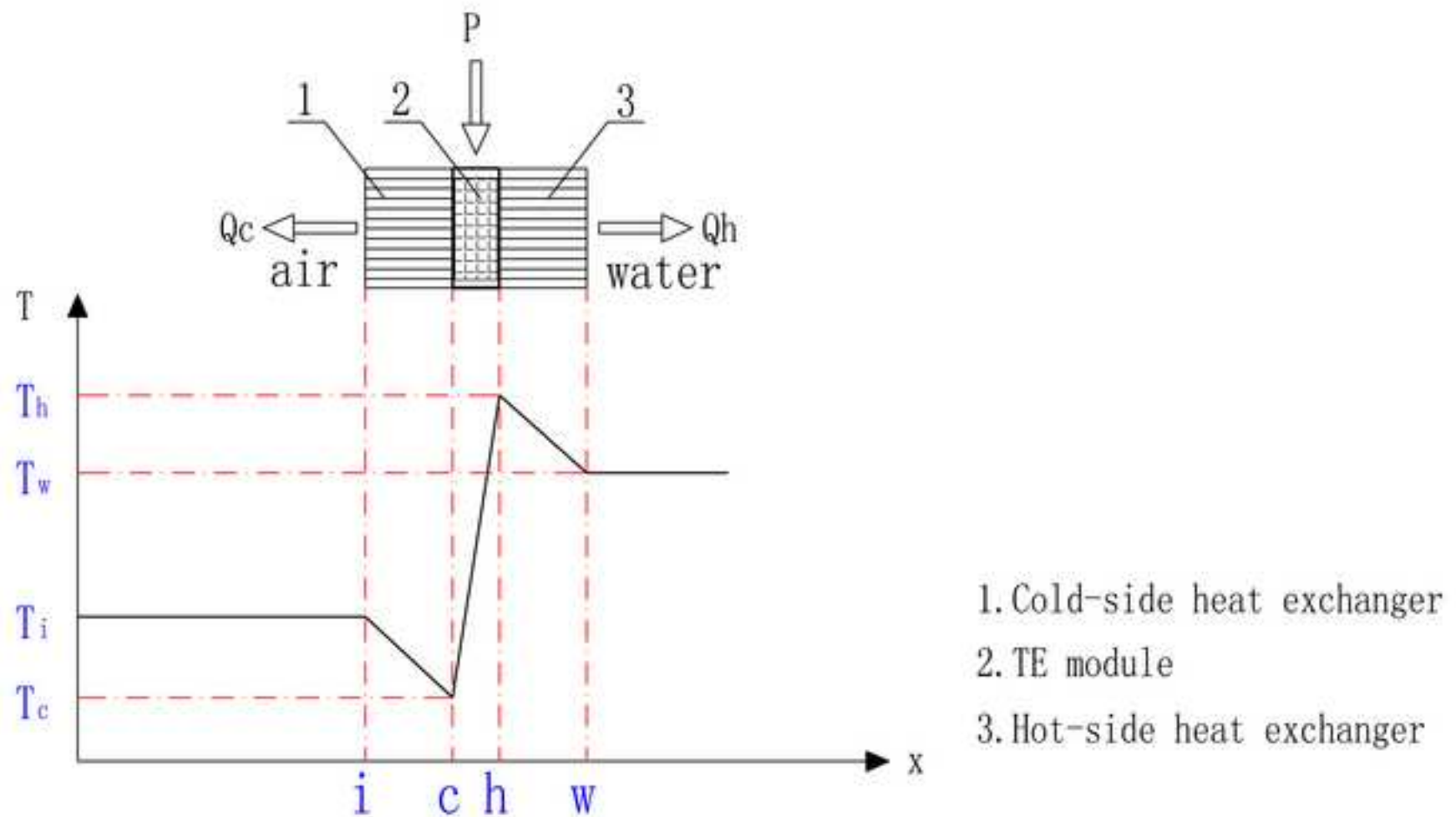
439 mode.

440

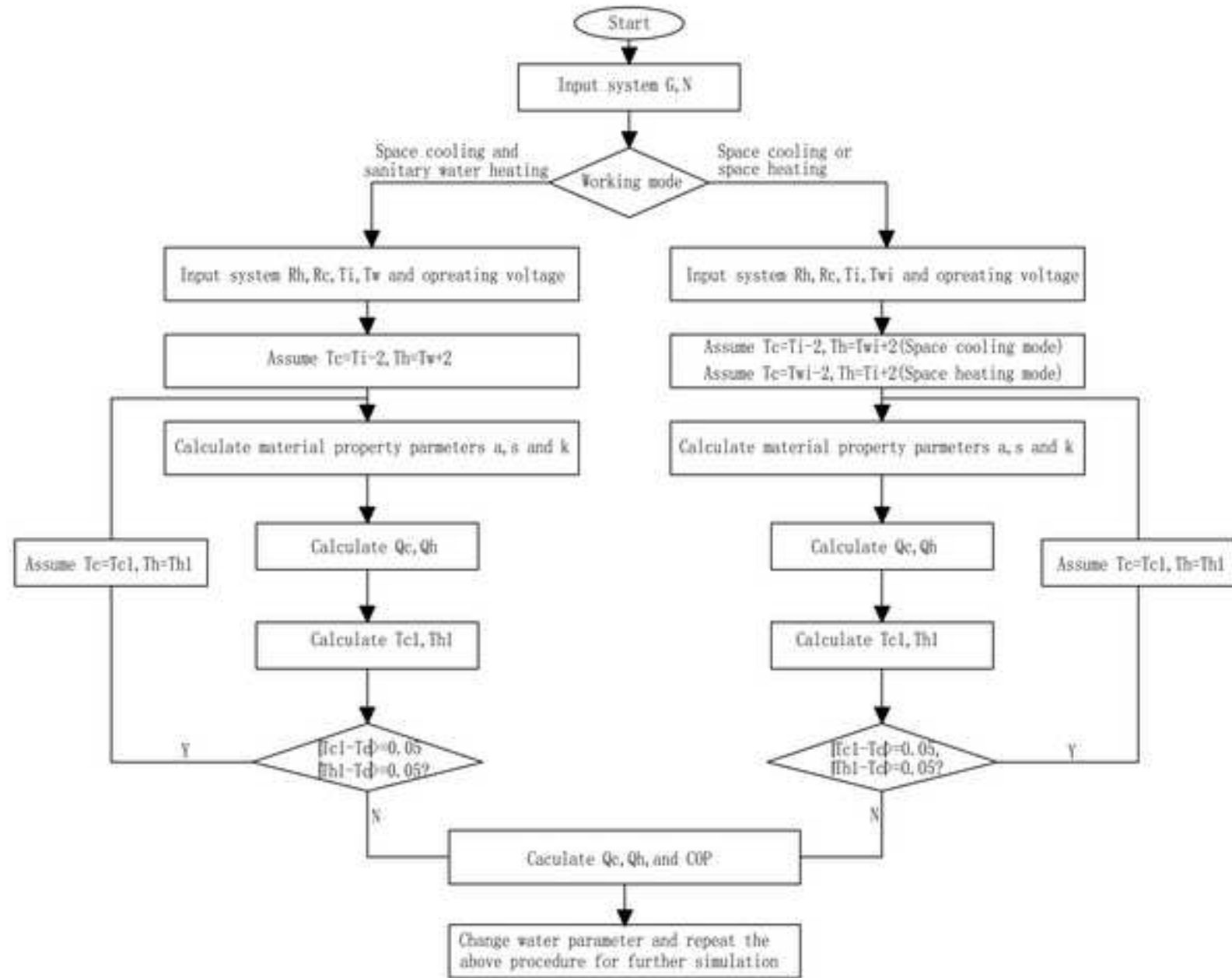
Figure(1)



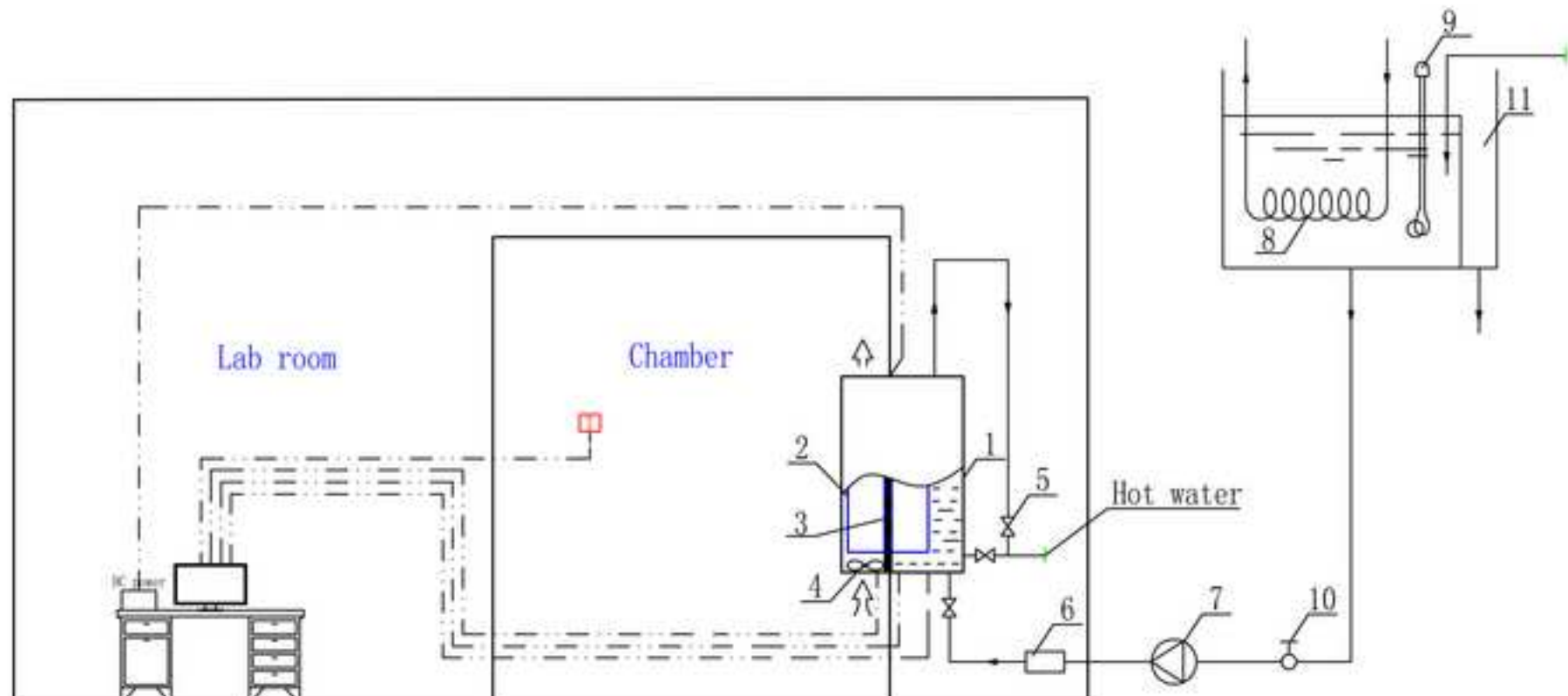
Figure(2)



Figure(3)

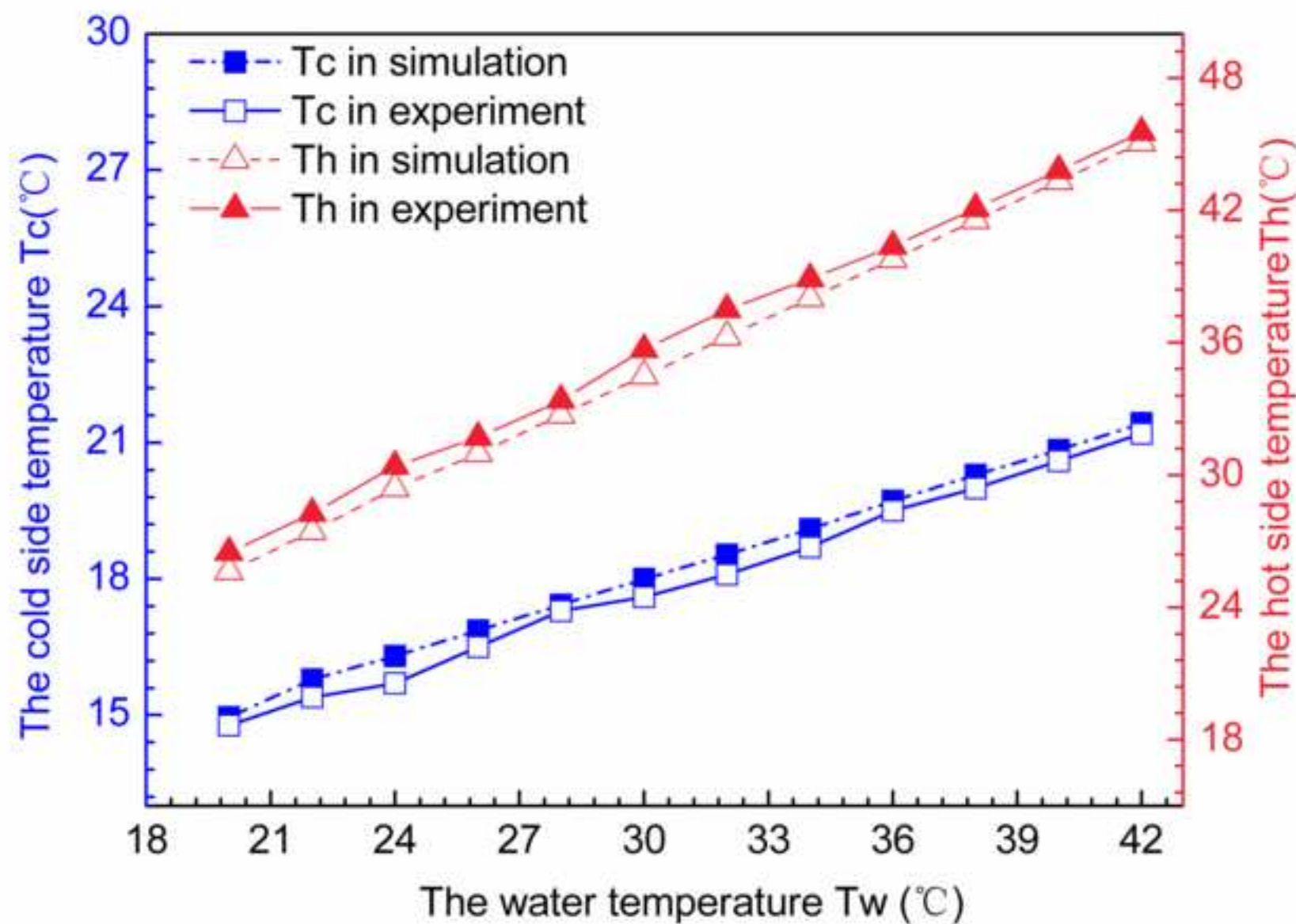


Figure(4)

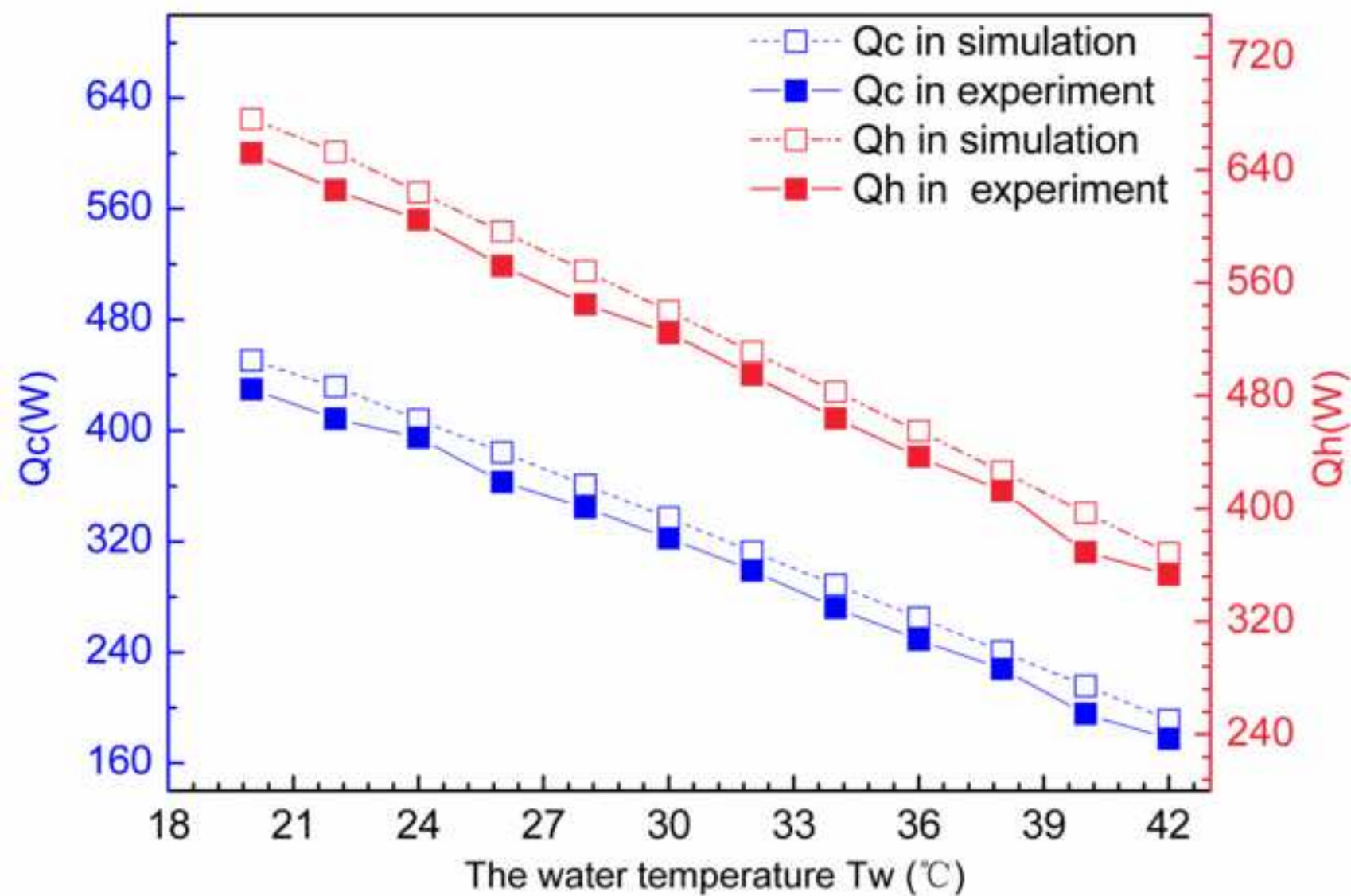


- 1. Water tank
- 2. Heat pipe exchanger
- 3. TE module
- 4. Fan
- 5. Motorized valve
- 6. Flow meter
- 7. Circulation pump
- 8. Copper coil for cooling
- 9. Pipe heater
- 10. Value for adjustment of cooling water flow rate
- 11. head tank

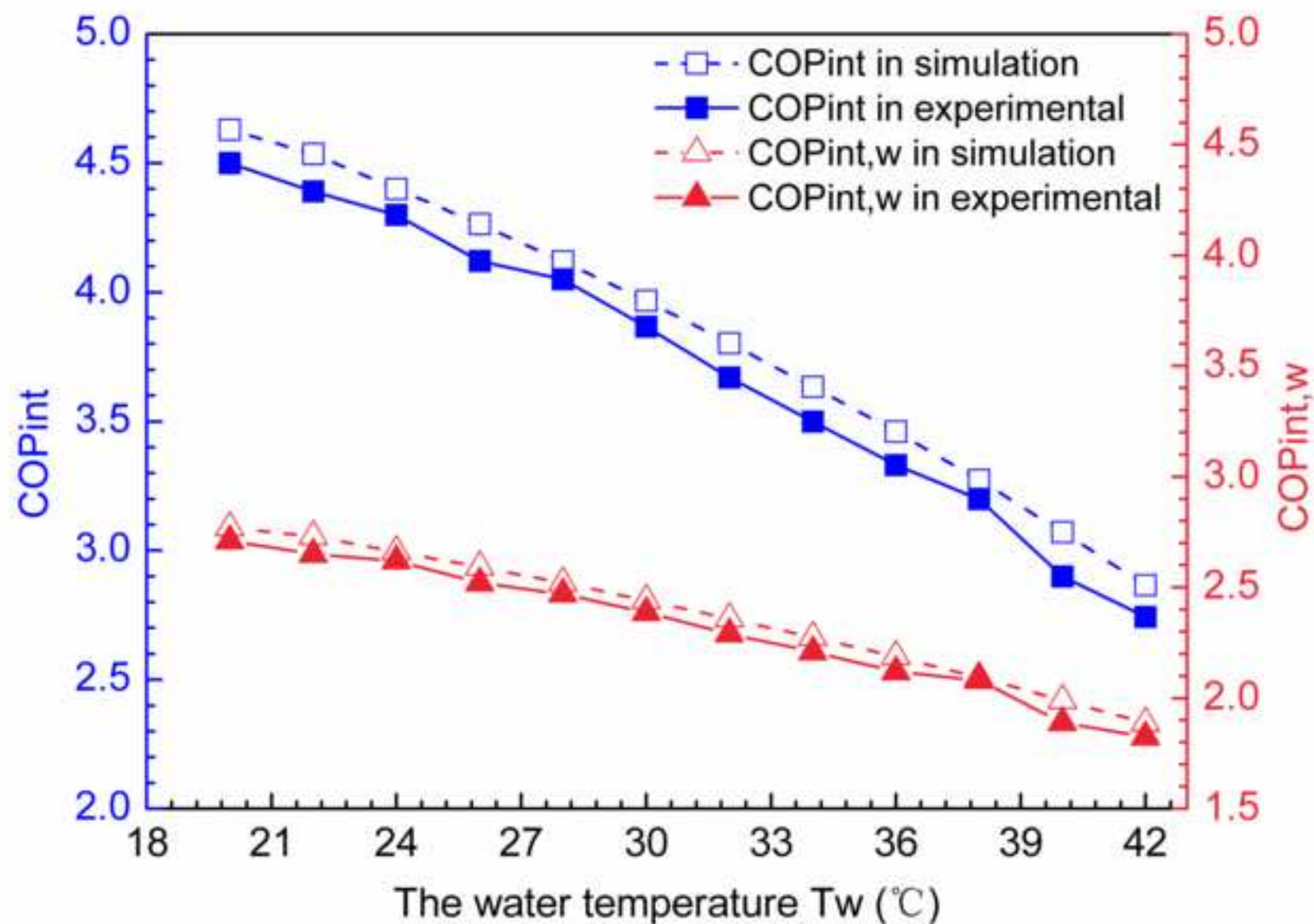
Figure(5)



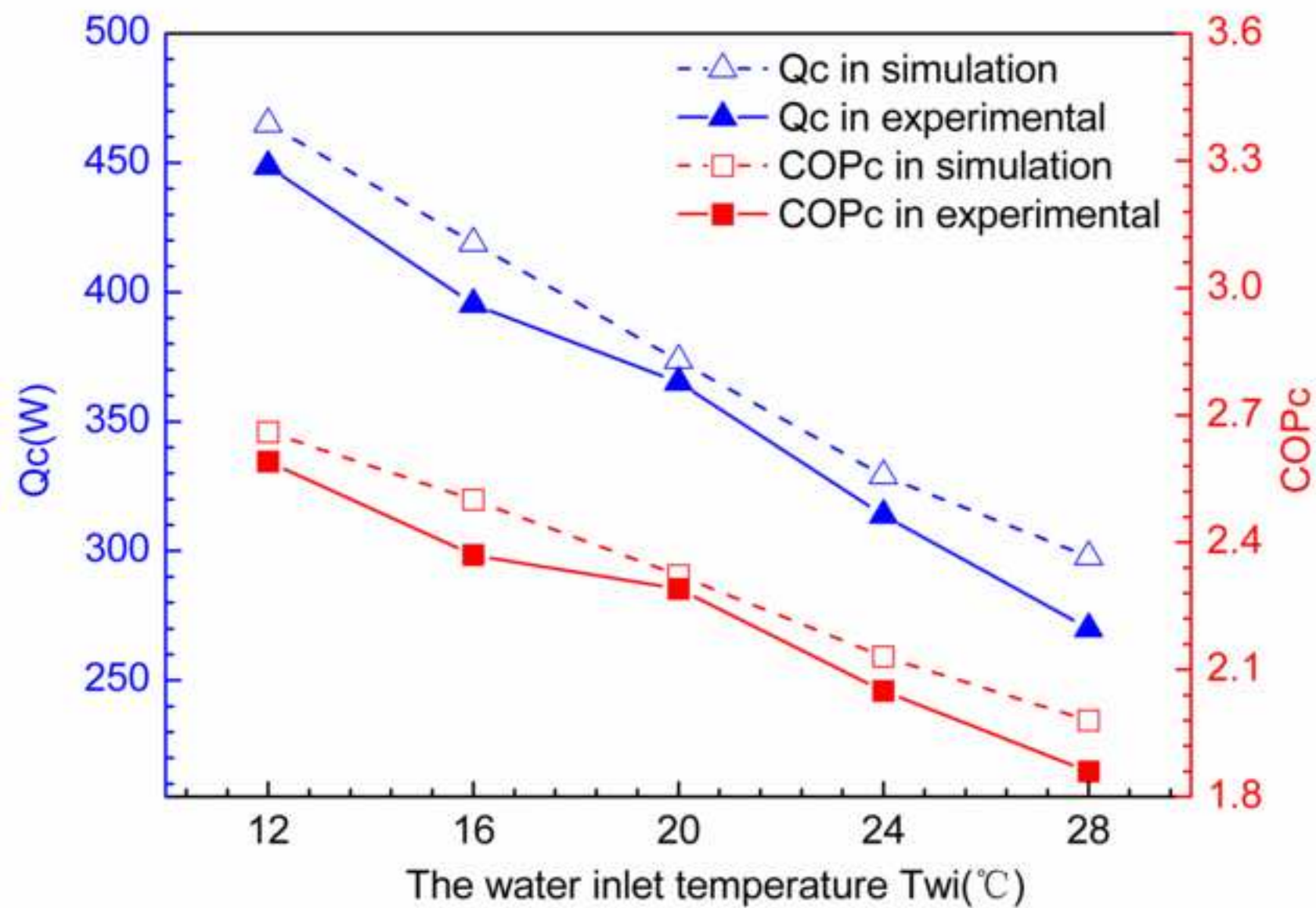
Figure(6)



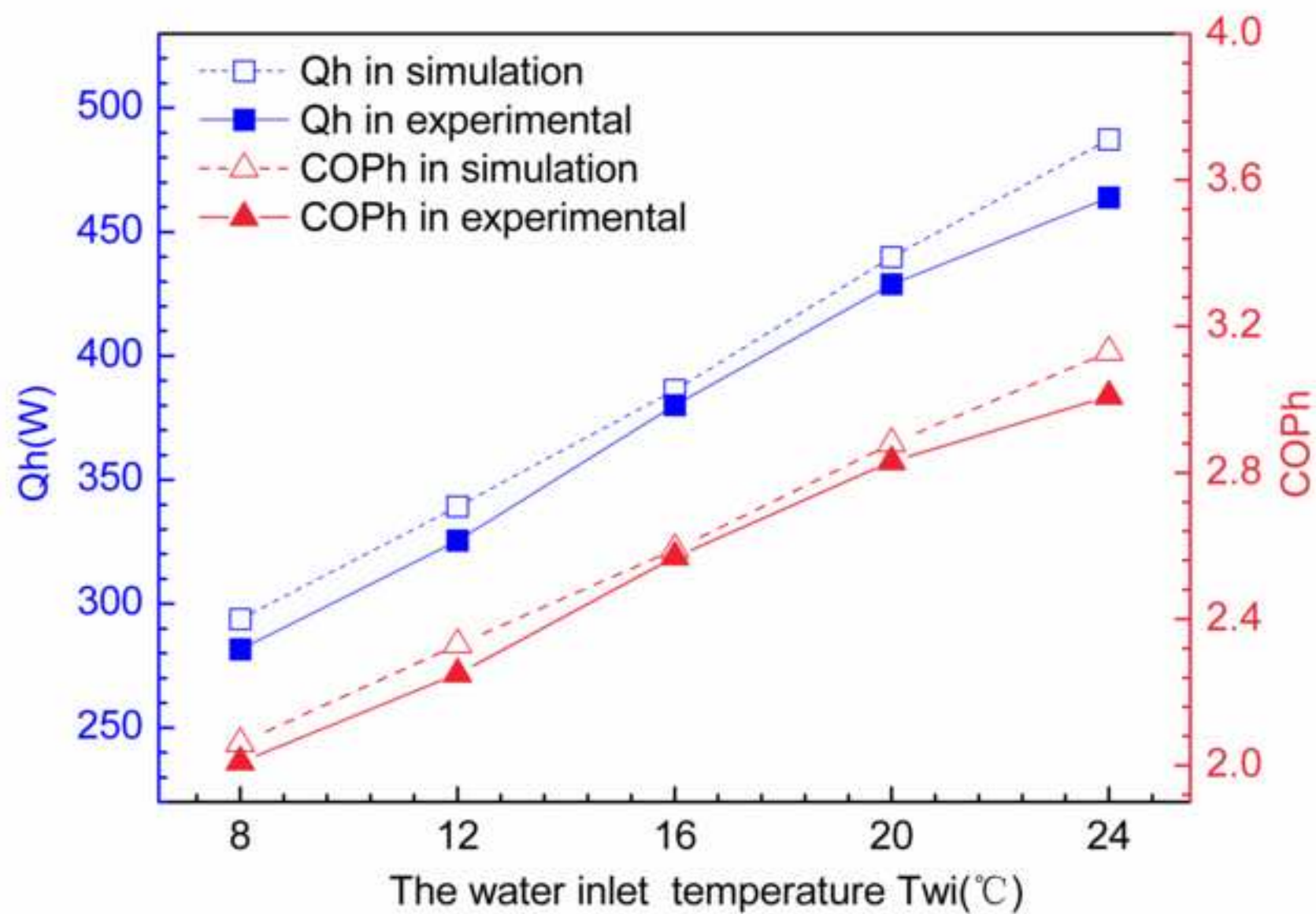
Figure(7)



Figure(8)



Figure(9)



Figure(10)

